

1 **Chemical variability in volcanic plumes and fumaroles along the East African**
2 **Rift System: new insights from the Western Branch**
3
4

5 **G. Boudoire^{1,2*}, G. Giuffrida², M. Liuzzo², N. Bobrowski^{3,4}, S. Calabrese^{2,5}, J. Kuhn^{3,4}, J.-C. Kazadi**
6 **Mwepu⁶, F. Grassa², S. Caliro⁷, A.L. Rizzo², F. Italiano², M. Yalire⁶, K. Karume⁶, A. Muhindo**
7 **Syavulisembo⁶, D. Tedesco^{7,8}**
8
9

10 ¹UCA, CNRS, IRD, OPGC, Laboratoire Magmas et Volcans, 6 avenue Blaise Pascal, 63178
11 Aubière, France

12 ²Istituto Nazionale di Geofisica e Vulcanologia, Sezione di Palermo, Italy

13 ³Institut für Umweltphysik, Ruprecht Karls University, Heidelberg, Germany

14 ⁴Max Planck Institut für Chemie, Mainz, Germany

15 ⁵DiSTeM, Università degli Studi di Palermo, Italy

16 ⁶Observatoire Volcanologique de Goma, Democratic Republic of Congo

17 ⁷Osservatorio Vesuviano, Istituto Nazionale di Geofisica e Vulcanologia, Naples, Italy

18 ⁸DISTABIF, Università degli Studi della Campania Luigi Vanvitelli, Italy
19

20 * Corresponding author. Present address: Laboratoire Magmas et Volcans, Campus universitaire
21 des Cézeaux, 6 Avenue Blaise Pascal, 63170 Aubière, France. Telephone : +33 (0)4 73 34 67 23.
22 E-mail : guillaume.boudoire@uca.fr.
23

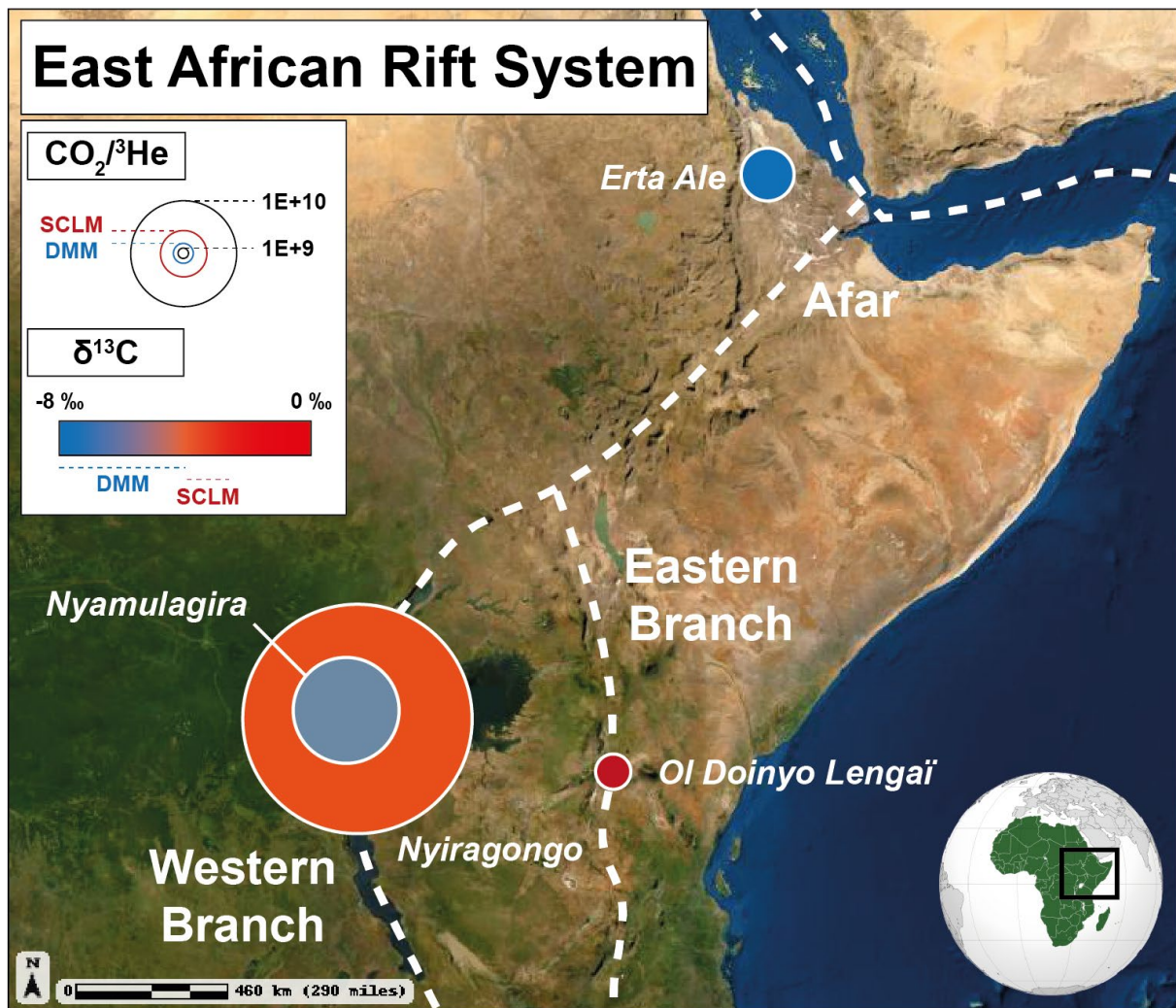
24 **Highlights:**

- 25 • Origin of volcanic CO₂ emissions along the East African Rift System
26 • Role of the Sub-Continental Lithospheric Mantle in the genesis of magmatic fluids beneath
27 the Virunga Volcanic Province
28 • Carbonate metasomatism of the mantle source
29

30 **Abstract**

31 The origin of magmatic fluids along the East African Rift System (EARS) is a long-lived field of
 32 debate in the scientific community. Here, we investigate the chemical composition of the volcanic
 33 plume and fumaroles at Nyiragongo and Nyamulagira (Democratic Republic of Congo), the only
 34 two currently erupting volcanoes set on the Western Branch of the rift. Our results are in line with
 35 earlier conceptual models proposing that volcanic gas emissions along the EARS mainly reflect
 36 variable contributions of the Sub-Continental Lithospheric Mantle (SCLM) and deeper fluids. At
 37 Nyiragongo and Nyamulagira, our study suggests that volcanic gas emissions preserve the
 38 fingerprint of the SCLM. High $\text{CO}_2/{}^3\text{He}$ in fumaroles of both volcanoes is thought to reflect
 39 carbonate metasomatism in the mantle source. As inferred by previous results obtained on the lava
 40 chemistry, this carbonate metasomatism would be more pronounced beneath Nyiragongo.

41

42 **Graphical abstract**

43

44 **Keywords:**

45 East African Rift System, volcano, gas chemistry

46

47 **1 Introduction**

48 The East African Rift System (EARS) is the longest active continental rift system on Earth and is
49 extensively studied by the scientific community focused on plate tectonics and geodynamics (e.g.,
50 Rooney et al., 2020) (Fig. 1). In the last few years, also the role of continental rifting on the global
51 carbon budget and climate dynamics has been revisited (Wong et al., 2019). Large diffusive CO₂
52 emissions together with the unusual abundance of carbon-rich melts are among many evidences
53 of the peculiarity of the EARS concerning the cycling of volatiles elements. However, the origin
54 of such volatile elements beneath the EARS remains understudied with respect to other
55 geodynamical contexts (Rooney et al., 2020). It has been firstly proposed that only the Afar-
56 Ethiopian part of the EARS shows the contribution of a deep common ('C'-type) mantle plume as
57 revealed by the abundance of primordial helium (³He/⁴He up to 19.6 Ra and mostly >9 Ra) (Pik et
58 al., 2006; Darrah et al., 2013; O'Connor et al., 2019; Rooney et al., 2020). The magmatic activity
59 along the Eastern and Western branches of the rift marked by lower ³He/⁴He values (<9 Ra) were
60 ascribed to the contribution of either a Depleted Morb Mantle 'DMM' (Fischer et al., 2009) or
61 distinct shallow mantle plumes upwelling (Pik et al., 2006). The discovery of ratios as high as 15
62 Ra in the Rungwe Volcanic Province in the South of Tanzania (Barry et al., 2013) upset this theory
63 and has favored the emergence of a new model in which gas emissions along the whole EARS
64 testify various extents of mixing between two components (Halldorsson et al., 2014; O'Connor et
65 al., 2019): (1) a deep Common ('C'-type) mantle plume (cf. "African Superplume") and (2) the
66 Sub-Continental Lithospheric Mantle 'SCLM'.

67 A field survey in the Virunga Volcanic Province (Democratic Republic of Congo) in 2020
68 allowed gas collection from volcanic plumes and fumaroles at Nyiragongo and Nyamulagira (Fig.
69 1), the only two currently erupting volcanoes on the Western Branch of the EARS (see Methods
70 in Supplementary Information). Based on the first chemical characterization of the fumaroles at
71 Nyamulagira, we explore here the current geochemical variability of gas emissions in this part of
72 the Virunga Volcanic Province (see Results in Supplementary Information; Fig. 2). By compiling
73 previous chemical data obtained from fumaroles and volcanic plumes at other persistently active
74 volcanoes along the EARS, we investigate the spatial variability of geochemical markers in
75 volcanic gaseous emissions along the EARS (Fig. 2).

76

77 **2 Samples and Methods**

78 The chemical characterization of volcanic gaseous plumes was performed by using a
79 Multicomponent Gas Analyzer System (MultiGAS) designed at the Istituto Nazionale di Geofisica
80 e Vulcanologia – Sezione di Palermo (INGV Palermo) (Aiuppa et al., 2006; Liuzzo et al., 2013).
81 The instrument allows the collection of H₂O, CO₂ and SO₂ contents in the plume with a 1 Hz
82 acquisition frequency. Two acquisition periods (>30 minutes) were realized at Nyamulagira on
83 February 4 and 6, 2020 and further two at Nyiragongo on February 12, 2020 (Fig. 1c, d). Time
84 series were then postprocessed to calculate CO₂/SO₂ and H₂O/CO₂ ratios with a typical uncertainty
85 <10%. Only ratios with a r-squared >0.7 on a period greater than 5 minutes were considered and
86 averaged to obtain final values for each volcanic plume (Table S-1).

87 One fumarolic gas sample (F2) was collected on February 4, 2020, within the Nyamulagira
88 summit crater with outlet temperature of 84°C (Fig. 1d). Similarly, two fumarolic gas samples (F1-
89 A & F1-B) were collected on February 12 and 13, 2020, on the second platform within the

90 Nyiragongo summit crater (for a description of the summit crater see e.g. Burgi et al., 2020) with
91 outlet temperature of 82°C (Fig. 1c). Glass samplers were used on line with a 50 cm stainless-steel
92 tube and Dewar glass tubes (Vaselli et al., 2006). Collected gas samples were then analyzed for
93 their contents in major and minor gaseous species as well as for the isotopic composition of noble
94 gases (^3He , ^4He , ^{20}Ne , ^{40}Ar , ^{38}Ar , ^{36}Ar) and their relative ratios, and few other stable isotopes ($\delta^{13}\text{C}$
95 of CO_2 , $\delta^{18}\text{O}$ and $\delta^2\text{D}$ of H_2O) (Table S-2). The analytical procedure and correction for air-
96 contamination of noble gases are the same as the ones described in Boudoire et al. (2020). In the
97 figures (Fig. 2, 3, 4, 5), the analytical uncertainty on laboratory measurements is less than the size
98 of the symbol.

99 Rain gauge collectors were deployed (i) beneath the volcanic plume at Nyamulagira (less
100 than <500 m distance to the plume emission center) during the field mission and (ii) at the
101 Observatoire Volcanologique de Goma more than 20 km further downwind (more details of the
102 sampling procedure are available in Calabrese et al. (2011)). Rainwater samples were collected to
103 investigate plume-rain interaction and define a Local Meteoric Water Line (LMWL) based on $\delta^{18}\text{O}$
104 and δD of H_2O . Stable isotopes for H_2O in both condensates from fumaroles (Table S-2) and
105 rainwaters (Table S-3) were analyzed at the Osservatorio Vesuviano (INGV) (see Brombach et al.
106 (2003) for details about the analytical procedure). Expected $\delta^{18}\text{O}$ value in local rain was calculated
107 from the equation of Bowen & Wilkinson (2002) with a latitude of 1° and an altitude of 3000 m
108 in accordance with the geographic position of the Nyamulagira volcano.

109 Previous data obtained in volcanic plumes and fumaroles at persistently active volcanoes
110 along the EARS are compiled from Gerlach (1982), Oppenheimer et al. (2002), Pik et al. (2006),
111 Sawyer et al. (2008a,b), Fischer et al. (2009), Tedesco et al. (2010), Darrah et al. (2013),
112 Bobrowski et al. (2017), Boucher et al. (2018) and Mollex et al. (2018). The composition of the
113 end-members (DMM, African Superplume, SCLM, Continental Crust, Oceanic Crust, Limestone,
114 Sediments, Mantle carbonates, Air and ASW) used to define the mixing curves are defined from
115 Sheppard & Epstein (1970), Harmer (1999), Gautheron & Moreira (2002), Pik et al. (2006),
116 Zelenski & Taran (2011), Barry et al. (2013), Clog et al., (2013), Hallis et al. (2015) and Taran &
117 Zelenski (2015), Casola et al. (2020).

118 **3 Results**

119 MultiGAS measurements in volcanic plumes performed in February 2020 reveal an average
120 CO_2/SO_2 ratio of 22 ± 8.4 and 15.5 ± 5.7 and an average $\text{H}_2\text{O}/\text{CO}_2$ ratio of 1.9 ± 0.2 and 12.4 ± 6.3 at
121 Nyiragongo and Nyamulagira, respectively (Fig. 2a). At Nyiragongo, CO_2/SO_2 values are higher
122 than FTIR measurements performed in the volcanic plume in 2005-2007 ($\text{CO}_2/\text{SO}_2 = 5.1\pm 0.1$;
123 $\text{H}_2\text{O}/\text{CO}_2 = 3.0\pm 0.2$; Sawyer et al., 2008a). At Nyamulagira, CO_2/SO_2 values are similar to those
124 obtained in the volcanic plume in 2014 with the same instrument but with a lower $\text{H}_2\text{O}/\text{CO}_2$ ratio,
125 on average ($\text{CO}_2/\text{SO}_2 = 12.1\pm 0.3$; $\text{H}_2\text{O}/\text{CO}_2 = 16.8\pm 0.1$; Bobrowski et al., 2017). Current and
126 previous data point out a CO_2/SO_2 range at Nyamulagira (9.7-21.1) overlapped by Nyiragongo's
127 one (5.0-29.1) while the $\text{H}_2\text{O}/\text{CO}_2$ range is clearly higher at Nyamulagira (9.6-19.6) than at
128 Nyiragongo (1.1-3.2). At larger scale, the ratios obtained for the two erupting volcanoes of the
129 Western branch of the EARS range between two endmembers: Erta Ale and Ardoukoba in the
130 Afar ($\text{CO}_2/\text{SO}_2 = 0.2-1.9$; $\text{H}_2\text{O}/\text{CO}_2 = 3.8-25.6$; Gerlach, 1982; Sawyer et al., 2008b) and Ol
131 Doinyo Lengai on the Eastern branch of the EARS ($\text{CO}_2/\text{SO}_2 = 3830$; $\text{H}_2\text{O}/\text{CO}_2 = 3.1$;
132 Oppenheimer et al., 2002).

133 N_2/He and N_2/Ar in fumaroles at Nyiragongo (F1-A and F1-B) range between 1885-1980
134 and 86-91, respectively. Higher values are set in fumarole (F2) at Nyamulagira with $\text{N}_2/\text{He} = 6814$

135 and $N_2/Ar = 93$. These values fall very well in what is expected for a mixture between either a
 136 DMM or a continental crust component and the air (Fig. 2b). They are intermediate between those
 137 measured at Erta Ale and Ol Doinyo Lengai.

138 Helium isotopes are indistinguishable in fumaroles of both volcanoes with R/Ra in the
 139 range 7.0-7.3 at Nyiragongo and 7.2 at Nyamulagira (Fig. 3a). These values set for both volcanoes
 140 of the Virunga Volcanic Province are lower than those observed in the Afar region ($R/Ra > 10.9$;
 141 Boucher et al., 2018; Darrah et al., 2013) but comparable to those of the Ol Doinyo Lengai (R/Ra
 142 = 6.6-7.8; Fischer et al., 2009; Mollex et al., 2018). They are at the limit between the lower range
 143 of DMM values ($R/Ra = 8 \pm 1$) and the upper range of the SCLM ($R/Ra = 6.1 \pm 0.9$; Gautheron &
 144 Moreira, 2002). $^4He/^{40}Ar^*$ ranges from 0.83 at Nyamulagira up to 1.24-1.41 at Nyiragongo, which
 145 is in accordance with previous measurements (1.02-1.20; Tedesco et al., 2010) and slightly higher
 146 than measured at Ol Doinyo Lengai (0.45-0.76; Fischer et al., 2009).

147 Carbon isotopes evidence the largest variability between the fumaroles of both volcanoes
 148 (Fig. 3b). At Nyiragongo, $\delta^{13}C$ of CO_2 range from -3.7 to -3.9 ‰ and are similar to previous
 149 measurements (from -3.5 to -4.0 ‰; Tedesco et al., 2010). More negative values are measured at
 150 Nyamulagira ($\delta^{13}C = -5.2$ ‰ in F2). With respect to preexisting measurements performed along
 151 the EARS, $\delta^{13}C$ values at Nyiragongo are close to those of Ol Doinyo Lengai (from -2.4 to -4.0
 152 ‰; Fischer et al., 2009) slightly more positive than typical DMM values (-6 ± 2 ‰; Sano & Marty,
 153 1995) and closer to the European SCLM values (-3.5 ‰; Bräuer et al., 2016; Rizzo et al., 2018).
 154 $\delta^{13}C$ values at Nyamulagira are closer to those measured at Erta Ale (from -6.3 to -6.8 ‰; Boucher
 155 et al., 2018) and fall in the range of DMM values.

156 $\delta^{18}O$ and δD measurements of H_2O of rainwaters collected less than 500 m-far from the
 157 plume emission center at Nyamulagira and at the Observatoire Volcanologique de Goma (more
 158 than 20 km-further) show a well-marked linear correlation ($\delta D = 8.08 \delta^{18}O + 20.07$; $R^2 = 0.996$),
 159 parallel to the Global Meteoric Water Line (GMWL), and could be representative of the Local
 160 Meteoric Water Line (LMWL) (Fig. 4). In this respect, the calculated local rain should have an
 161 isotopic composition of $\delta^{18}O = -11.1$ ‰ and $\delta D = -69.4$ ‰ (Bowen & Wilkinson, 2002). $\delta^{18}O$ and
 162 δD measurements of H_2O performed in the condensate fraction of the Nyamulagira fumaroles
 163 (only) range from 7.2 to 8.4 ‰ and from -34.4 to -34.7 ‰, respectively. These values are far from
 164 the LMWL and quite similar to SCLM inferred values (Fig. 4; Taran & Zelenski, 2015).

165

166 4. Discussion

167 4.1. Contribution of the SCLM beneath the Virunga Volcanic Province

168 Recent attempts to describe the geochemical variability along the EARS, especially in gaseous
 169 emissions, refer mainly to various extents of mixing between a deep Common ('C'-type) mantle
 170 plume (cf. "African Superplume") and a SCLM (Halldorsson et al., 2014; Mollex et al., 2018;
 171 O'Connor et al., 2019) component. In this frame, measurements obtained in the Afar (Erta Ale,
 172 Dallol) are ascribed to a greater contribution of the mantle plume (Darrah et al., 2013; Boucher et
 173 al., 2018) whereas the activity on the Eastern Branch (Ol Doinyo Lengai) is thought representative
 174 of the predominant contribution of the SCLM in the genesis of magmatic fluids (Mollex et al.,
 175 2018).

176 Rc/Ra in the range 7.1-7.5 at both Nyiragongo and Nyamulagira volcanoes may reflect (i)
 177 a DMM signature (8 ± 1) or (ii) a SCLM-like signature (6.1 ± 0.9) marked by a slight enrichment in
 178 3He (Fig. 3a). Actually, $\delta^{13}C$ values of CO_2 at Nyiragongo (Fig. 3b) and $\delta^{18}O$ and δD
 179 measurements of H_2O at Nyamulagira are rather similar to what expected from the contribution of
 180 the SCLM in the genesis of magmatic fluids (Fig. 4), as proposed at the Ol Doinyo Lengai on the

181 other branch of the EARS (Mollex et al., 2018). The composition of the volcanic gas plumes (H₂O
 182 – CO₂ – S_i; Fig. 2a) at both Nyamulagira and Nyiragongo is also strongly different than that
 183 measured during the 1978 Ardoukoba eruption fed by E-MORB magma (Vigier et al., 1999).

184 Our results match with previous conclusions from petrological investigations along the
 185 Western Branch of the EARS that discard a predominant contribution of a DMM source in the
 186 genesis of magmatic fluids there (Rosenthal et al., 2009; Rooney et al., 2020). Conversely, partial
 187 involvement of deeper mantellic fluids may provide a reasonable explanation to the slight
 188 enrichment in primordial helium (³He) in gaseous emissions at both Nyiragongo (Rc/Ra = 7.1-7.4
 189 and up to 8.7 in previous studies) and Nyamulagira (Rc/Ra = 7.5) with respect to typical SCLM
 190 values (6.1±0.9). Mantle reservoirs at the origin of such an enrichment in ³He in the SCLM may
 191 involve indistinguishably: an undegassed archetypal mantle plume like the African Superplume
 192 (Darrah et al., 2013), a partially degassed mantle plume component as proposed in the Afar (Erta
 193 Ale; Darrah et al., 2013; Boucher et al., 2018) and/or a depleted mantle component (see Rooney
 194 et al. (2020) for a review). Further work is required to distinguish the influence of the components
 195 beneath the province.

196

197 **4.2. Carbon enrichment tracked by gaseous emissions**

198 The composition of the fumaroles in the Virunga Volcanic Province strongly differs from those
 199 sampled along the EARS when looking at CO₂/³He values. At Nyamulagira, CO₂/³He = 1.0 x 10¹⁰
 200 and ranges from 2.2 to 2.3 x 10¹⁰ at Nyiragongo. These values are almost one order of magnitude
 201 higher than measured in Ol Doinyo Lengai emissions representative of the SCLM beneath the
 202 Eastern Branch of the EARS (Fig. 5a). Considering the emission of natrocarbonatites at the Ol
 203 Doinyo Lengai volcano and the hyperalkaline nature of the cogenetic nephelinitic melts (Fischer
 204 et al., 2009), such an increase of the CO₂/³He seems hardly reconcilable with a differential CO₂-
 205 He solubility effect in alkaline melts. The absence of significant ⁴He/⁴⁰Ar* increase neither
 206 sustains the effect of equilibrium degassing in the increase of CO₂/³He (Burnard et al., 2004) as
 207 suggested in some gaseous emissions at Dallol (cf. Gr. I on Fig. S-1; Darrah et al., 2013). High
 208 CO₂/³He in gas emissions at Nyamulagira and Nyiragongo are rather ascribed to various extent of
 209 mixing with either (i) a hosted sediment-limestone crustal source (Darrah et al., 2013) or (ii)
 210 mantellic carbonates as observed in other continental rift systems (Frezzotti & Touret, 2014).

211 The absence of important change of δ¹³C values at high CO₂/³He with respect to the SCLM
 212 (Fig. 5b) minimizes the likelihood of (i) the influence of an interaction with crustal sediment or
 213 limestone as proposed at Dallol (Darrah et al., 2013) or evidenced in regional hot springs (Tedesco
 214 et al., 2010). Once again, (ii) the presence of carbonate-bearing metasomes in the SCLM source
 215 derived from deeper fluids, as extensively documented along the Western Branch of the EARS
 216 (Rooney et al., 2020; Aiuppa et al., 2021), may provide a reasonable explanation to such a CO₂/³He
 217 increase at quite constant δ¹³C (-1 to -8 ‰ for primary carbonatites; Harmer, 1999; Casola et al.,
 218 2020). This hypothesis is sustained by the chemistry of lavas emitted at Nyiragongo and
 219 Nyamulagira that points out limited contamination processes at crustal levels and rather
 220 emphasizes carbonate metasomatism in the mantle source beneath Nyiragongo (Chakrabarti et al.,
 221 2009; Pouclet et al., 2016; Aiuppa et al., 2021).

222

223 **4.3. Potential sources of heterogeneities between gaseous emissions at Nyiragongo and 224 Nyamulagira**

225 If the composition of fumaroles at both Nyiragongo and Nyamulagira (12 km far away only) share
 226 common features with respect to other volcanic emissions along the EARS, both present distinct

227 $\delta^{13}\text{C}$ signature of CO_2 and $\text{CO}_2/{}^3\text{He}$ values (Fig. 3 and 4). We identified three potential scenarios
228 that might account for such chemical variability.

229 In the first scenario ('1' on Fig. 5), a process of Rayleigh fractional condensation (about 50
230 %) of CO_2 during the ascent of the gas phase up to the surface (Mook et al., 1974) could account
231 for (i) the lowest $\text{CO}_2/{}^3\text{He}$ and $\delta^{13}\text{C}$ values and (ii) the enrichment in less condensable gas species
232 such as He, Ne, Ar (Table S-2) observed at Nyamulagira with respect to Nyiragongo. This process
233 was extensively documented in peripheral "cold" dry CO_2 -rich emission so-called "mazukus"
234 located on the edge of the Lake Kivu (Fig. 1; Tedesco et al., 2010). However, this process suggests
235 a common source of magmatic fluids at both volcanoes (similar initial $\text{CO}_2/{}^3\text{He}$ and $\delta^{13}\text{C}$ of CO_2
236 before condensation) that hardly reconciliates the variations observed in the chemistry of "high
237 temperature" volcanic plumes between both volcanoes (Fig. 2a; Bobrowski et al., 2017) and in the
238 lava chemistry (Chakrabarti et al., 2009; Pouclet et al., 2016).

239 In the second scenario ('2' on Fig. 5), the composition of the fumaroles at Nyamulagira
240 represent a mixing between mantle fluids similar to those emitted at Nyiragongo (80%) and fluids
241 from a partially degassed mantle component as proposed in the Afar (20%). The analysis of
242 halogen elements in volcanic plumes at both Nyamulagira and Nyiragongo also suggests a better
243 affinity of the former with the volcanic plume at Erta Ale (Bobrowski et al., 2017). However, lava
244 isotopic chemistry rather supports the opposite scenario: the (Sr-Nd-Pb) isotopic composition of
245 lavas at Nyiragongo ranges intermediate between those at the Nyamulagira volcano and the
246 Common ('C'-type) mantle plume component described in the Afar region (Chakrabarti et al.,
247 2009; Rooney et al., 2020).

248 In the third scenario ('3' on Fig. 5), a small addition (<0.1 %) of recycled sediments could
249 explain the more negative $\delta^{13}\text{C}$ values at Nyamulagira with respect to those at Nyiragongo. This
250 recycled component may be either (i) intrinsic to the mantle source through the involvement of a
251 recycled crustal material as suggested by the isotopic composition of lavas at Nyamulagira
252 (Chakrabarti et al., 2009) or (ii) shallower, i.e., related to the interaction with metasediments at
253 crustal level or organic matter close to the surface like observed at Dallol (e.g., transition from Gr.
254 I to Gr. II; Darrah et al., 2013). In both cases, the involvement of a biogenic and potentially
255 hydrated component could provide one explanation to the (H_2O - CO_2 -S_i) affinity of the volcanic
256 plume of Nyamulagira with the range of composition defined by arc volcanism (Fig. 2a; Burton et
257 al., 2000; Aiuppa et al., 2017).

258 We recognize that further work is required to better identify the origin of the heterogeneity
259 in gaseous emissions between both volcanoes. Meanwhile, it is worth noting that the last two
260 scenarios required an initially lower $\text{CO}_2/{}^3\text{He}$ at Nyamulagira ($< 1.2 \times 10^{10}$; Fig. 5b) that agrees
261 with a lesser extent of carbonate metasomatism in the mantle source beneath Nyamulagira
262 following the above discussion (Chakrabarti et al., 2009; Pouclet et al., 2016) where both
263 Nyamulagira and Nyiragongo lavas are ascribed to a mantle source incorporating preferentially
264 either a recycled crustal component or a carbonated component, respectively.

265

266 **5 Conclusions**

267 Fumaroles and volcanic plume sampling was conducted in February 2020 at the neighboring
268 Nyamulagira and Nyiragongo volcanoes in the Virunga Volcanic Province along the Western
269 Branch of the EARS. The isotope chemistry of the fumaroles and the composition of the volcanic
270 plume suggests the contribution of the Sub-Continental Lithospheric Mantle (SCLM) in the

271 genesis of volcanic fluids beneath the area. CO₂/³He measured at both volcanoes is higher than
272 values reported for other persistently active volcanoes along the EARS and suggests carbonate
273 metasomatism in the mantle source, especially beneath Nyiragongo. This result is consistent with
274 the chemical investigation of lavas performed in the area and more globally with the presence of
275 numerous mantle metasomes beneath the Western Branch of the EARS. Heterogeneities between
276 gaseous emissions at Nyiragongo and Nyamulagira mainly relate to the composition of the
277 volcanic plume and the δ¹³C of the CO₂ in fumaroles. We stress that such variability could reflect
278 the influence of a biogenic and/or more hydrated component expressed in volcanic fluids at
279 Nyamulagira.

280

281 **Acknowledgments, Samples, and Data**

282 We are grateful to the Goma Volcano Observatory (OVG) for the invitation and logistic help.
283 MONUSCO is warmly thanked for the great support in the field deployment by helicopter. The
284 ICCN is acknowledged for providing the logistic inside the National Parc of Virunga. The Swiss
285 team is thanked for their priceless support in the logistics of the descent into the craters. We are in
286 debt with Y. Oliveri (INGV), F. Salerno (INGV), and M. Tantillo (INGV), for their assistance
287 during gas analysis in laboratory. This research was financed by the Italian INGV initiative
288 LakeCarb and the French government IDEX-ISITE initiative 16-IDEX-0001 (CAP 20-25) through
289 the project CarbSol. Data discussed in this study are fully available in Supplementary Information.
290

291 **References**

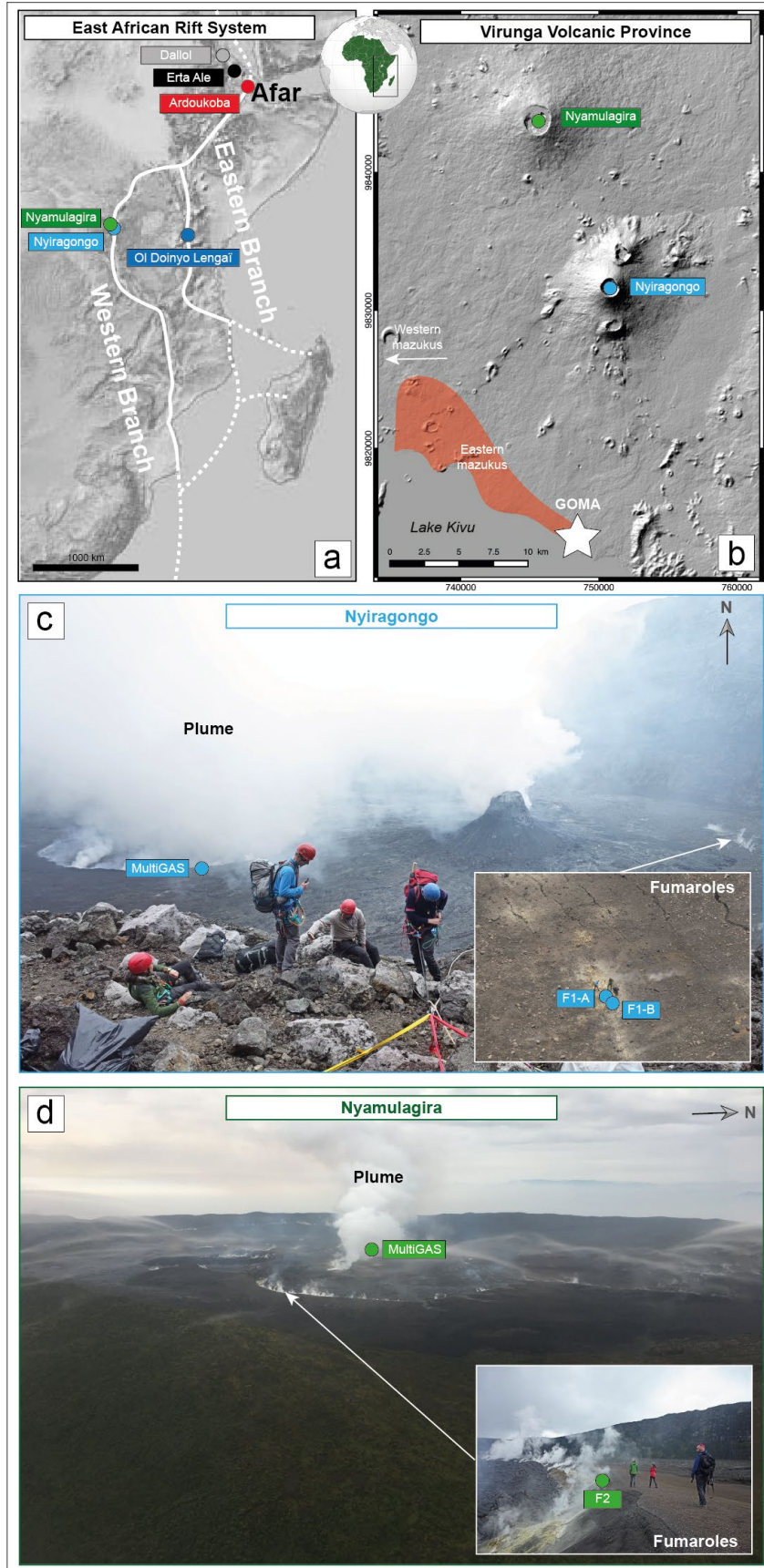
- 292 Aiuppa A., Federico C., Giudice G., Gurrieri S., Liuzzo M., Shinohara H., Favara R. & Valenza
293 M. (2006). Rates of carbon dioxide plume degassing from Mount Etna volcano. *J. Geophys. Res.*,
294 111, B09207, doi:10.1029/2006JB004307.
- 295
- 296 Aiuppa, A., Fischer, T. P., Plank, T., Robidoux, P., & Di Napoli, R. (2017). Along-arc, inter-arc
297 and arc-to-arc variations in volcanic gas CO₂/ST ratios reveal dual source of carbon in arc
298 volcanism. *Earth-Science Reviews*, 168, 24-47.
- 299
- 300 Allard, P., Tazieff, H., & Dajlevic, D. (1979). Observations of seafloor spreading in Afar during
301 the November 1978 fissure eruption. *Nature*, 279(5708), 30-33.
- 302
- 303 Barry, P. H., Hilton, D. R., Fischer, T. P., De Moor, J. M., Mangasini, F., & Ramirez, C. (2013).
304 Helium and carbon isotope systematics of cold “mazuku” CO₂ vents and hydrothermal gases and
305 fluids from Rungwe Volcanic Province, southern Tanzania. *Chemical Geology*, 339, 141-156.
- 306
- 307 Bobrowski, N., Giuffrida, G. B., Yalire, M., Lübcke, P., Arellano, S., Balagizi, C., Calabrese, S.,
308 Galle, B., & Tedesco, D. (2017). Multi-component gas emission measurements of the active lava
309 lake of Nyiragongo, DR Congo. *Journal of African Earth Sciences*, 134, 856-865.
- 310
- 311 Boucher, C., Lan, T., Marty, B., Burnard, P. G., Fischer, T. P., Ayalew, D., Mabry, J., Maarten de
312 Moor, J., Zelenski, M.E., & Zimmermann, L. (2018). Atmospheric helium isotope composition as

- 313 a tracer of volcanic emissions: A case study of Erta Ale volcano, Ethiopia. *Chemical Geology*,
314 480, 3-11.
- 315
- 316 Boudoire, G., Rizzo, A. L., Arienzo, I., & Di Muro, A. (2020). Paroxysmal eruptions tracked by
317 variations of helium isotopes: inferences from Piton de la Fournaise (La Réunion island). *Scientific*
318 *reports*, 10(1), 1-16.
- 319
- 320 Bowen, G. J., & Wilkinson, B. (2002). Spatial distribution of $\delta^{18}\text{O}$ in meteoric
321 precipitation. *Geology*, 30(4), 315-318.
- 322
- 323 Bräuer, K., Geissler, W. H., Kämpf, H., Niedermann, S., & Rman, N. (2016). Helium and carbon
324 isotope signatures of gas exhalations in the westernmost part of the Pannonian Basin (SE
325 Austria/NE Slovenia): Evidence for active lithospheric mantle degassing. *Chemical Geology*, 422,
326 60-70.
- 327
- 328 Brombach, T., Caliro, S., Chiodini, G., Fiebig, J., Hunziker, J. C., & Raco, B. (2003). Geochemical
329 evidence for mixing of magmatic fluids with seawater, Nisyros hydrothermal system,
330 Greece. *Bulletin of Volcanology*, 65(7), 505-516.
- 331
- 332 Burgi, P. Y., Boudoire, G., Rufino, F., Karume, K., & Tedesco, D. (2020). Recent activity of
333 Nyiragongo (Democratic Republic of Congo): New insights from field observations and numerical
334 modeling. *Geophysical Research Letters*, 47(17), e2020GL088484.
- 335
- 336 Burnard, P., Graham, D., & Farley, K. (2004). Fractionation of noble gases (He, Ar) during MORB
337 mantle melting: a case study on the Southeast Indian Ridge. *Earth and Planetary Science*
338 *Letters*, 227(3-4), 457-472.
- 339
- 340 Burton, M. R., Oppenheimer, C., Horrocks, L. A., & Francis, P. W. (2000). Remote sensing of
341 CO_2 and H_2O emission rates from Masaya volcano, Nicaragua. *Geology*, 28(10), 915-918.
- 342
- 343 Calabrese, S., Aiuppa, A., Allard, P., Bagnato, E., Bellomo, S., Brusca, L., D'Alessandro, W., &
344 Parello, F. (2011). Atmospheric sources and sinks of volcanogenic elements in a basaltic volcano
345 (Etna, Italy). *Geochimica et Cosmochimica Acta*, 75(23), 7401-7425.
- 346
- 347 Casola, V., France, L., Galy, A., Bouden, N., & Villeneuve, J. (2020). No evidence for carbon
348 enrichment in the mantle source of carbonatites in eastern Africa. *Geology*, 48(10), 971-975.
- 349
- 350 Chakrabarti, R., Basu, A. R., Santo, A. P., Tedesco, D., & Vaselli, O. (2009). Isotopic and
351 geochemical evidence for a heterogeneous mantle plume origin of the Virunga volcanics, Western
352 rift, East African Rift system. *Chemical Geology*, 259(3-4), 273-289.
- 353
- 354 Clog, M., Aubaud, C., Cartigny, P., & Dosso, L. (2013). The hydrogen isotopic composition and
355 water content of southern Pacific MORB: A reassessment of the D/H ratio of the depleted mantle
356 reservoir. *Earth and Planetary Science Letters*, 381, 156-165.
- 357

- 358 Darrah, T. H., Tedesco, D., Tassi, F., Vaselli, O., Cuoco, E., & Poreda, R. J. (2013). Gas chemistry
359 of the Dallol region of the Danakil Depression in the Afar region of the northern-most East African
360 Rift. *Chemical Geology*, 339, 16-29.
- 361
362 Fischer, T. P., Burnard, P., Marty, B., Hilton, D. R., Füre, E., Palhol, F., Sharp, Z.D., & Mangasini,
363 F. (2009). Upper-mantle volatile chemistry at Oldoinyo Lengai volcano and the origin of
364 carbonatites. *Nature*, 459(7243), 77-80.
- 365
366 Frezzotti, M. L., & Touret, J. L. (2014). CO₂, carbonate-rich melts, and brines in the
367 mantle. *Geoscience Frontiers*, 5(5), 697-710.
- 368
369 Gautheron, C., & Moreira, M. (2002). Helium signature of the subcontinental lithospheric
370 mantle. *Earth and Planetary Science Letters*, 199(1-2), 39-47.
- 371
372 Gerlach, T. M. (1982). Interpretation of volcanic gas data from tholeiitic and alkaline mafic lavas.
373 *Bulletin Volcanologique*, 45(3), 235-244.
- 374
375 Halldórsson, S. A., Hilton, D. R., Scarsi, P., Abebe, T., & Hopp, J. (2014). A common mantle
376 plume source beneath the entire East African Rift System revealed by coupled helium-neon
377 systematics. *Geophysical Research Letters*, 41(7), 2304-2311.
- 378
379 Hallis, L. J., Huss, G. R., Nagashima, K., Taylor, G. J., Halldórsson, S. A., Hilton, D. R., Motti,
380 M.J., & Meech, K. J. (2015). Evidence for primordial water in Earth's deep
381 mantle. *Science*, 350(6262), 795-797.
- 382
383 Harmer, R. E. (1999). The petrogenetic association of carbonatite and alkaline magmatism:
384 constraints from the Spitskop Complex, South Africa. *Journal of Petrology*, 40(4), 525-548.
- 385
386 Liuzzo, M., Gurrieri, S., Giudice, G., & Giuffrida, G. (2013). Ten years of soil CO₂ continuous
387 monitoring on Mt. Etna: Exploring the relationship between processes of soil degassing and
388 volcanic activity. *Geochemistry, Geophysics, Geosystems*, 14(8), 2886-2899.
- 389
390 Mollex, G., Füre, E., Burnard, P., Zimmermann, L., Chazot, G., Kazimoto, E. O., Marty, B., &
391 France, L. (2018). Tracing helium isotope compositions from mantle source to fumaroles at
392 Oldoinyo Lengai volcano, Tanzania. *Chemical Geology*, 480, 66-74.
- 393
394 Mook, W. G., Bommerson, J. C., & Staverman, W. H. (1974). Carbon isotope fractionation
395 between dissolved bicarbonate and gaseous carbon dioxide. *Earth and Planetary Science
396 Letters*, 22(2), 169-176.
- 397
398 O'Connor, J. M., Jokat, W., Regelous, M., Kuiper, K. F., Miggins, D. P., & Koppers, A. A. (2019).
399 Superplume mantle tracked isotopically the length of Africa from the Indian Ocean to the Red Sea.
400 *Nature communications*, 10(1), 1-13.
- 401

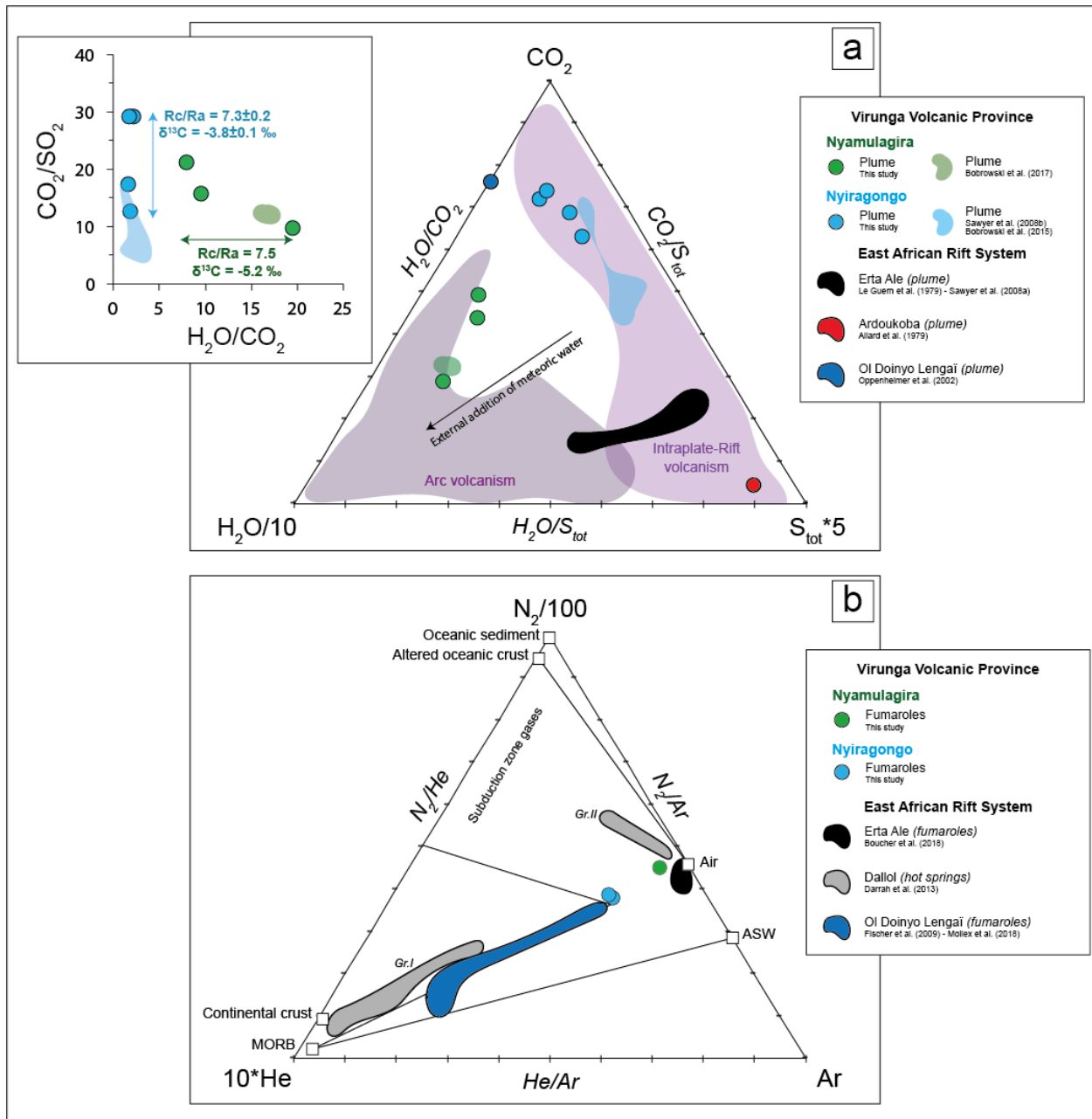
- 402 Oppenheimer, C., Burton, M. R., Durieux, J., & Pyle, D. M. (2002). Open-path Fourier transform
403 spectroscopy of gas emissions from Oldoinyo Lengai volcano, Tanzania. *Optics and lasers in*
404 *engineering*, 37(2-3), 203-214.
- 405
- 406 Pik, R., Marty, B., & Hilton, D. R. (2006). How many mantle plumes in Africa? The geochemical
407 point of view. *Chemical Geology*, 226(3-4), 100-114.
- 408
- 409 Pouclet, A., Bellon, H., & Bram, K. (2016). The Cenozoic volcanism in the Kivu rift: Assessment
410 of the tectonic setting, geochemistry, and geochronology of the volcanic activity in the South-Kivu
411 and Virunga regions. *Journal of African Earth Sciences*, 121, 219-246.
- 412 Rizzo, A. L., Pelorosso, B., Coltorti, M., Ntaflos, T., Bonadiman, C., Matusiak-Małek, M.,
413 Italiano, F., & Bergonzoni, G. (2018). Geochemistry of noble gases and CO₂ in fluid inclusions
414 from lithospheric mantle beneath Wilcza Góra (Lower Silesia, southwest Poland). *Frontiers in*
415 *Earth Science*, 6, 215.
- 416
- 417 Rooney, T. O. (2020). The Cenozoic magmatism of East Africa: part V—magma sources and
418 processes in the East African Rift. *Lithos*, 360, 105296.
- 419
- 420 Rosenthal, A., Foley, S. F., Pearson, D. G., Nowell, G. M., & Tappe, S. (2009). Petrogenesis of
421 strongly alkaline primitive volcanic rocks at the propagating tip of the western branch of the East
422 African Rift. *Earth and Planetary Science Letters*, 284(1-2), 236-248.
- 423
- 424 Sano, Y., & Marty, B. (1995). Origin of carbon in fumarolic gas from island arcs. *Chemical Geology*,
425 119, 265-274.
- 426
- 427 Sawyer, G. M., Carn, S. A., Tsanev, V. I., Oppenheimer, C., & Burton, M. (2008a). Investigation
428 into magma degassing at Nyiragongo volcano, Democratic Republic of the Congo. *Geochemistry,*
429 *Geophysics, Geosystems*, 9(2).
- 430
- 431 Sawyer, G. M., Oppenheimer, C., Tsanev, V. I., & Yirgu, G. (2008b). Magmatic degassing at
432 Erta'Ale volcano, Ethiopia. *Journal of Volcanology and Geothermal Research*, 178(4), 837-846.
- 433
- 434 Sheppard, S. M., & Epstein, S. (1970). D/H and ¹⁸O/¹⁶O ratios of minerals of possible mantle or
435 lower crustal origin. *Earth and Planetary Science Letters*, 9(3), 232-239.
- 436
- 437 Taran, Y., & Zelenski, M. (2015). Systematics of water isotopic composition and chlorine content
438 in arc-volcanic gases. *Geological Society, London, Special Publications*, 410(1), 237-262.
- 439
- 440 Tedesco, D., Tassi, F., Vaselli, O., Poreda, R. J., Darrah, T., Cuoco, E., & Yalire, M. M. (2010).
441 Gas isotopic signatures (He, C, and Ar) in the Lake Kivu region (western branch of the East
442 African rift system): Geodynamic and volcanological implications. *Journal of Geophysical*
443 *Research: Solid Earth*, 115(B1).
- 444
- 445 Vaselli, O., Tassi, F., Montegrossi, G., Capaccioni, B., & Giannini, L. (2006). Sampling and
446 analysis of volcanic gases. *Acta Vulcanologica*, 18(1/2), 67.

- 447
448 Vigier, N., Bourdon, B., Joron, J. L., & Allegre, C. J. (1999). U-decay series and trace element
449 systematics in the 1978 eruption of Ardoukoba, Asal rift: timescale of magma crystallization.
450 *Earth and Planetary Science Letters*, 174(1-2), 81-98.
- 451
452 Wong, K., Mason, E., Brune, S., East, M., Edmonds, M., & Zahirovic, S. (2019). Deep carbon
453 cycling over the past 200 million years: a review of fluxes in different tectonic settings. *Frontiers*
454 *in Earth Science*, 7, 1-22.
- 455
456 Zelenski, M., & Taran, Y. (2011). Geochemistry of volcanic and hydrothermal gases of Mutnovsky
457 volcano, Kamchatka: evidence for mantle, slab and atmosphere contributions to fluids of a typical
458 arc volcano. *Bulletin of Volcanology*, 73(4), 373-394.



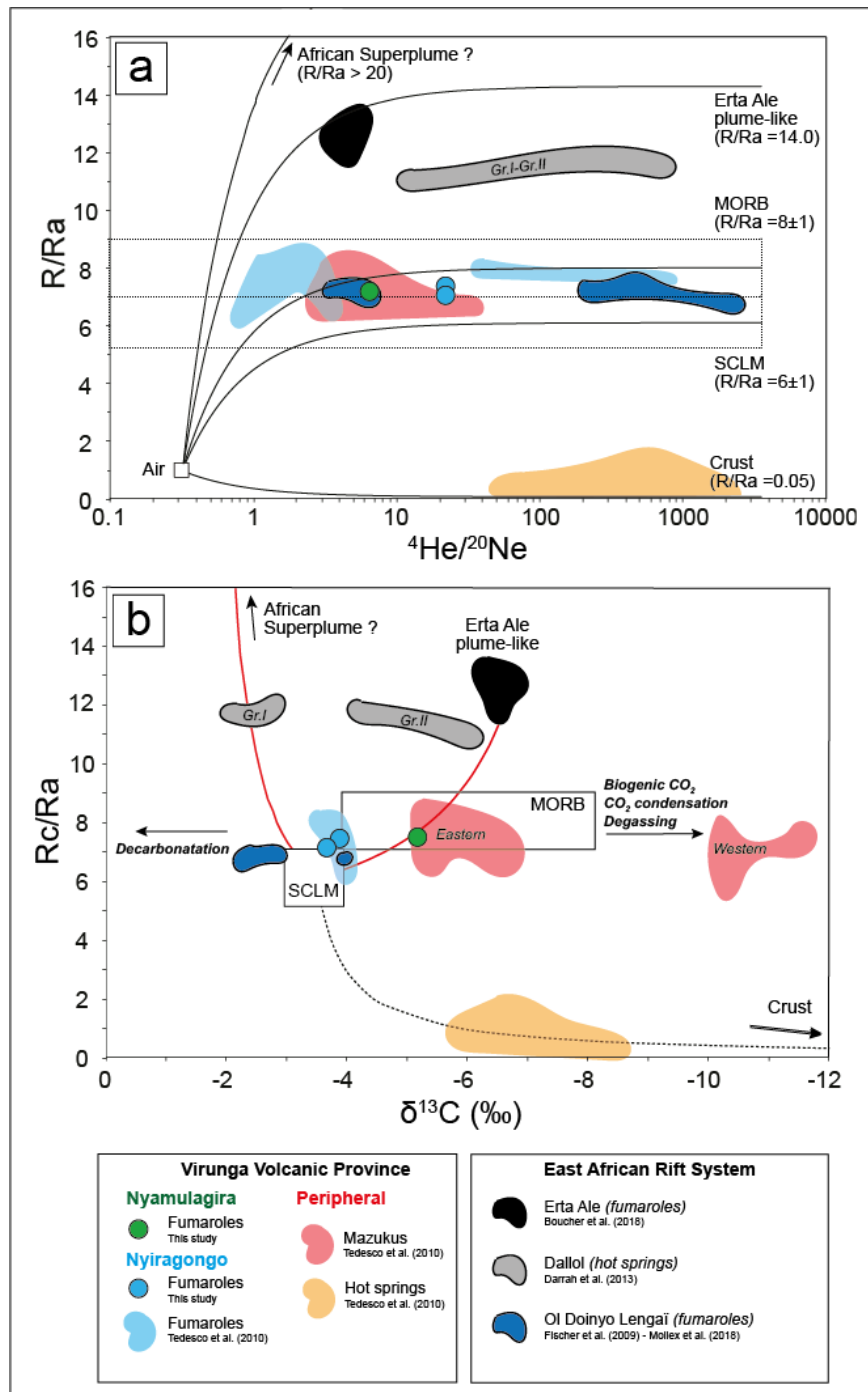
460 **Fig. 1** Location of volcanoes currently in eruption (plus the 1978 Ardoukoba eruption) (a) along the EARS
 461 and (b) in the Virunga Volcanic Province. The area of the cold dry CO₂-rich emission so-called
 462 “mazukus” are indicated in red (Tedesco et al., 2010). Volcanic plume and fumaroles sampling sites
 463 at (c) Nyiragongo and (d) Nyamulagira.

464



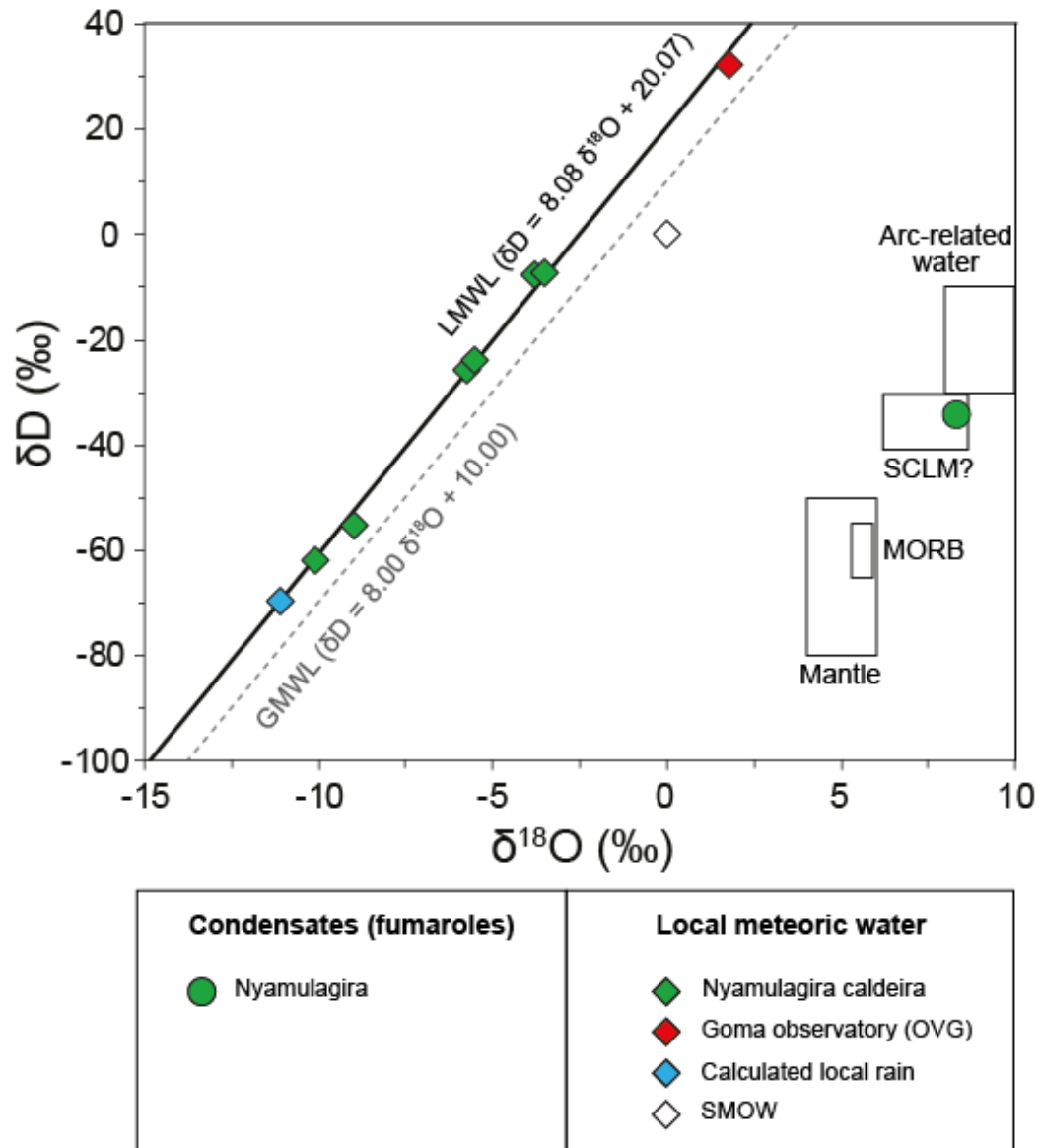
465

466 **Fig. 2** (a) MultiGAS measurements performed in the volcanic plume of Nyiragongo and
 467 Nyamulagira during the 2020 field mission. Rc/Ra and $\delta^{13}\text{C}$ values from fumaroles (inlay). (b) N₂-
 468 He-Ar ternary diagram of fumaroles composition along the EARS. Gr.I and Gr.II are the two
 469 distinct chemical groups of gas emissions identified at Dallol (Darrah et al., 2013).
 470



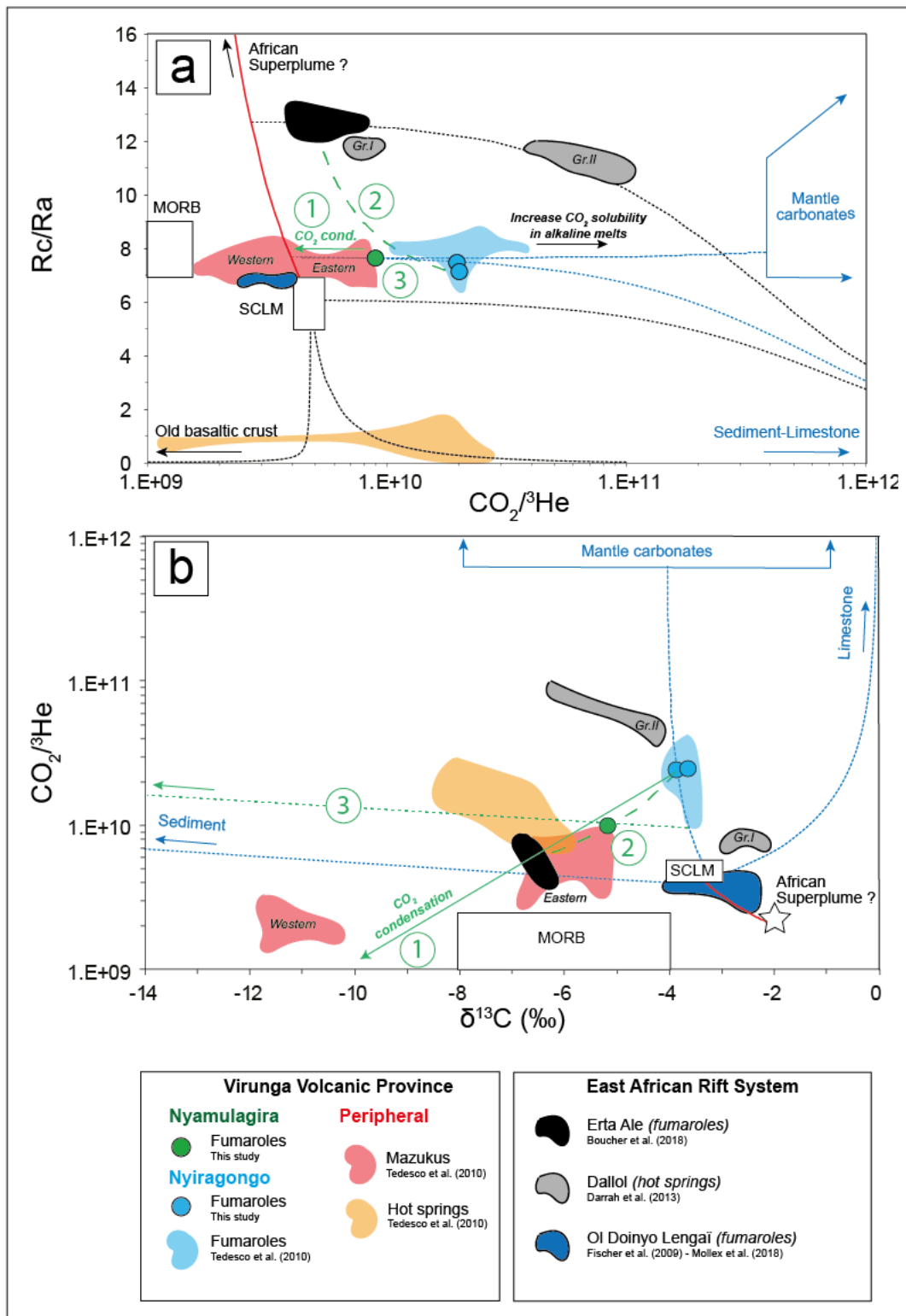
471

472 **Fig. 3** (a) $^4\text{He}/^{20}\text{Ne}$ vs. R/Ra . Black lines for mixing between the air and terrestrial end-members.
 473 (b) $\delta^{13}\text{C}$ vs. Rc/Ra . Red continuous lines for mixing between potential mantle plume-like
 474 components and the SCLM. Black dashed lines for mixing between SCLM and crustal components
 475 as testified by the chemical composition of the gas emissions from hot springs in the Virunga
 476 Volcanic Province (Tedesco et al., 2010).



477
478
479

480 **Fig. 4** Isotopic composition ($\delta^{18}\text{O}$ and $\delta^2\text{D}$ of H_2O) of condensates from fumaroles at
481 Nyamulagira and local rainwater samples collected beneath the volcanic plume at Nyamulagira
482 and at the Observatoire Volcanologique de Goma. The Local Meteoric Water Line is calculated
483 from the collected rainwater samples (see Methods for details).
484



485

486 **Fig. 5** (a) $\text{CO}_2/{}^3\text{He}$ vs. Rc/Ra and (b) $\delta^{13}\text{C}$ vs. $\text{CO}_2/{}^3\text{He}$. Continuous red line for mixing between
 487 an “African Superplume” component and the SCLM. Black and blue dotted lines for mixing with
 488 distinct crustal components or mantle carbonates (blue dotted lines are those discussed in the text)

489 about the geochemical variability of gaseous emissions in the Virunga Volcanic Province with
490 respect to the EARS). Green continuous, dotted and dashed lines relate to scenarios 1-2-3
491 discussed in the text and accounting for the chemical variability of gaseous emissions between
492 Nyamulagira and Nyiragongo. CO₂ condensation process from Mook et al. (1974) computed with
493 a temperature of 80°C similar to that measured in the fumaroles at Nyamulagira.
494